

Cut-Through Metal Slit Array as an Anisotropic Metamaterial Film

Jonghwa Shin, *Student Member, IEEE*, Jung-Tsung Shen, Peter B. Catrysse, *Member, IEEE*, and Shanhui Fan, *Senior Member, IEEE*

(Invited Paper)

Abstract—It has been shown that a metal film with a one-dimensional array of subwavelength cut-through slits can be accurately modeled as an anisotropic and uniform metamaterial film with nondispersive electric permittivity $[\bar{\epsilon}]$ and magnetic permeability $[\bar{\mu}]$ tensors. This model has an interesting scaling property: The values for the thickness L can be chosen at arbitrarily, provided that $[\bar{\epsilon}]$ and $[\bar{\mu}]$ are scaled accordingly. The analytical expressions of the corrections due to near fields have also been given. This framework provides an intuitive and precise model for the understanding of the metal slit arrays in the subwavelength regime.

Index Terms—Anisotropic material, metal slit, optical metamaterial, subwavelength resonance.

I. INTRODUCTION

STRUCTURES with a period less than the wavelength of light can have electromagnetic properties very different from those of their constituent materials. In particular, periodic metallic structures with subwavelength features have been actively researched in the recent years. The subwavelength resonances in these structures are responsible for their unique properties as novel metamaterials. Notable examples include effective plasmons in media [1]–[7], three-dimensional metallic crystals [8], negative refractive index [9]–[13], and spoof plasmons on metal surfaces [14].

Recently, it was shown that a metal slab of finite thickness with subwavelength cut-through slits (Fig. 1) can be regarded as a new metamaterial system [15]. In this system with thickness L , which is not necessarily subwavelength, the slits are filled with a nonmetallic material with an electric permittivity ϵ_c and a magnetic permeability μ_c . When the slit width a is sufficiently narrow compared to the subwavelength period d , it was shown that all electromagnetic properties of the system can be accurately described using a simple, isotropic, nonmagnetic ($\mu = 1$) model with a large dielectric constant that is frequency independent [15]. In fact, the model and the exact analytical description of the same system asymptotically approach each other in the limit $d/a \rightarrow \infty$. For smaller d/a ratios ($\lesssim 4$), it was

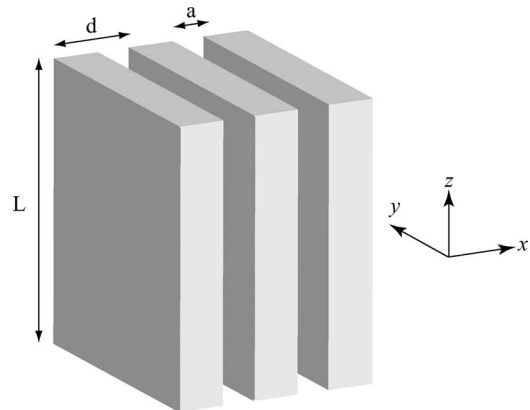


Fig. 1. Metal slit array system and coordinates.

also shown that the isotropic model starts to deviate from the exact analytical description [15].

Given that the slit structure is anisotropic, a natural step further is to consider an anisotropic metamaterial model. Here, we introduce the appropriate anisotropic model, where the system is described by an electric permittivity tensor $[\bar{\epsilon}]$ and a magnetic permeability tensor $[\bar{\mu}]$ that are both frequency independent. The model coincides with the isotropic one in [15] when $d/a \rightarrow \infty$. In addition, it also provides a very good description of the system even when d/a is small, in which case the isotropic model is no longer valid. It has also been shown that there in fact exists a whole class of anisotropic models that are equivalent to one another, if the thickness of the layer in the model is allowed to vary. The model is verified by comparing it to the analytic solution of the metal slit array, and the difference between the two is quantified.

II. ANISOTROPIC MODEL

The goal is to describe the structure shown in Fig. 1 with a uniform effective medium. With the choice of the coordinate system in Fig. 1, each axis lies on a high-symmetry direction of the structure. The diagonal forms for the effective electric permittivity and magnetic permeability tensors can be assumed as

$$[\bar{\epsilon}] = \begin{pmatrix} \bar{\epsilon}_x & 0 & 0 \\ 0 & \bar{\epsilon}_y & 0 \\ 0 & 0 & \bar{\epsilon}_z \end{pmatrix} \quad [\bar{\mu}] = \begin{pmatrix} \bar{\mu}_x & 0 & 0 \\ 0 & \bar{\mu}_y & 0 \\ 0 & 0 & \bar{\mu}_z \end{pmatrix}. \quad (1)$$

Manuscript received December 1, 2005; revised April 20, 2006. This work was supported in part by the National Science Foundation under Grant ECS-0134607 and in part by the Air Force Office of Scientific Research under Grant FA9550-04-1-0437.

The authors are with the Edward L. Ginzton Laboratory, Stanford University, Stanford, CA 94305 USA (e-mail: shanhui@stanford.edu).

Digital Object Identifier 10.1109/JSTQE.2006.879577

Following [15], which showed that the main effect arises from the existence of a subwavelength propagating mode in the slits, the primary focus here is on the transverse magnetic (TM) polarization. This polarization has the electric field (\mathbf{E} field) in the zx plane, and the magnetic field (\mathbf{H} field) parallel to the y direction. Thus, the only relevant parameters for this polarization are $\bar{\epsilon}_x$, $\bar{\epsilon}_z$, and $\bar{\mu}_y$. (For the rest of the paper, variables with a bar are assumed to be quantities related to the effective medium.)

A. Derivation of an Anisotropic Model

For the moment, it is assumed that the effective medium has the same thickness as the real system ($\bar{L} = L$). It will be shown that the following relations regarding the effective medium hold:

$$\begin{aligned}\bar{\epsilon}_x &= d/a \\ \bar{\epsilon}_z &= \infty \\ \bar{\mu}_y &= a/d \\ \bar{L} &= L.\end{aligned}\quad (2)$$

(A similar conclusion has been reached for a different system consisting of a periodic arrangement of parallel grooves in a metal substrate [16]. Here, we focus on cut-through slits.) These equations are deduced by finding the effective indices (\bar{n}_{xy} and \bar{n}_{zy}) and the effective impedance ($\bar{\eta}$). \bar{n}_{xy} (\bar{n}_{zy}) is the effective index for the polarization, where the \mathbf{E} field is in the $x(z)$ direction and the \mathbf{H} field is in the y direction.

The effective refractive indices can be derived by comparing the field configurations inside the metal slits with those inside the effective medium. For a TM wave with a given frequency (ω) and a given tangential wavenumber (k_x), the fields inside a metal slit can be formulated as follows:

$$\begin{aligned}H_y &= H_{y0} e^{ik_z z} \\ E_x &= \frac{k_z}{\omega \epsilon_c} H_{y0} e^{ik_z z} \\ E_z &= 0.\end{aligned}\quad (3)$$

The above is in fact the transverse electromagnetic (TEM) mode of a rectangular metallic waveguide, which is the only propagating mode inside the slit in the subwavelength regime. In contrast, inside the effective medium, the most general form for a TM wave can be expressed as

$$\begin{aligned}\bar{H}_y &= \bar{H}_{y0} e^{i\bar{k}_z z} e^{ik_x x} \\ \bar{E}_x &= \frac{\bar{k}_z}{\omega \bar{\epsilon}_x} \bar{H}_{y0} e^{i\bar{k}_z z} e^{ik_x x} \\ \bar{E}_z &= \frac{-k_x}{\omega \bar{\epsilon}_z} \bar{H}_{y0} e^{i\bar{k}_z z} e^{ik_x x}.\end{aligned}\quad (4)$$

An important feature of the metal slit system is that E_z is zero inside the slits. To have zero \bar{E}_z inside the effective medium as well, $\bar{\epsilon}_z$ needs to be infinite. Another important feature of (3) is that the field inside a slit is independent of k_x . Consequently, the dispersion relation

$$\omega^2 = \frac{k_z^2 c^2}{\epsilon_c \mu_c} \equiv \frac{k_z^2 c^2}{n_c^2} \quad (5)$$

where c is the speed of light, is also independent of k_x . Comparing (5) with the dispersion relation of the anisotropic effective medium

$$\omega^2 = \frac{\bar{k}_z^2 c^2}{\bar{\epsilon}_x \bar{\mu}_y} + \frac{k_x^2 c^2}{\bar{\epsilon}_z \bar{\mu}_y} \equiv \frac{\bar{k}_z^2 c^2}{\bar{n}_{xy}^2} + \frac{k_x^2 c^2}{\bar{n}_{zy}^2} \quad (6)$$

one can immediately observe that the two dispersion relations can be made to have the same form, provided that again we set $\bar{\epsilon}_z = \infty$. Then, the dispersion relations become

$$\begin{aligned}k_z c &= \omega \sqrt{\epsilon_c \mu_c} \\ \bar{k}_z c &= \omega \sqrt{\bar{\epsilon}_x \bar{\mu}_y}.\end{aligned}\quad (7)$$

In addition, assuming that the length of the effective medium is the same as the length of the physical medium ($\bar{L} = L$), and the phase accumulation over the thickness of the structure is the same ($\bar{k}_z \bar{L} = k_z L$), the transverse effective index is obtained as

$$\sqrt{\bar{\epsilon}_x \bar{\mu}_y} = \sqrt{\epsilon_c \mu_c} \quad \text{i.e., } \bar{n}_{xy} = n_c. \quad (8)$$

Equation (8) gives only the product of $\bar{\mu}_y$ and $\bar{\epsilon}_x$. To determine them individually, their ratio is also needed. This ratio is the square of the effective transverse impedance. This impedance can be calculated from the continuity conditions across the interface between the structure and the surrounding medium, for the tangential \mathbf{E} field and the normal component of Poynting vector. The continuity of the tangential \mathbf{E} field is a direct result of the Maxwell's equations, and the continuity of the normal component of the Poynting vector comes from the steady-state assumption and the energy conservation law. The continuity of these quantities between the surrounding medium and the system, whether the system is the metallic structure or the effective medium, requires that the quantities should be the same for the metallic structure and the effective medium at the interface. By matching the average tangential \mathbf{E} field (E_x) in (3) and (4), we get

$$\frac{\bar{k}_z}{\omega \bar{\epsilon}_x} \bar{H}_{y0} = \frac{a}{d} \frac{k_z}{\omega \epsilon_c} H_{y0}. \quad (9)$$

By matching the average normal Poynting vector, we get

$$\frac{\bar{k}_z}{\omega \bar{\epsilon}_x} |\bar{H}_{y0}|^2 = \frac{a}{d} \frac{k_z}{\omega \epsilon_c} |H_{y0}|^2. \quad (10)$$

From (7), (9), and (10), we conclude that

$$\sqrt{\frac{\bar{\mu}_y}{\bar{\epsilon}_x}} = \frac{a}{d} \sqrt{\frac{\mu_c}{\epsilon_c}} \quad \text{i.e., } \bar{\eta} = \frac{a}{d} \eta_c. \quad (11)$$

Thus, based on first-principle and heuristic considerations, we now have a complete knowledge of the effective medium for the TM polarization: The effective impedance ($\bar{\eta}$) and indices (\bar{n}_{xy} and \bar{n}_{zy}), or, equivalently, the effective electric permittivities ($\bar{\epsilon}_x$ and $\bar{\epsilon}_z$) and magnetic permeability ($\bar{\mu}_y$), as described in (2).

B. Test of the Anisotropic Model

This anisotropic model, though simple, provides a very accurate description of the system for d/a ratios from infinity

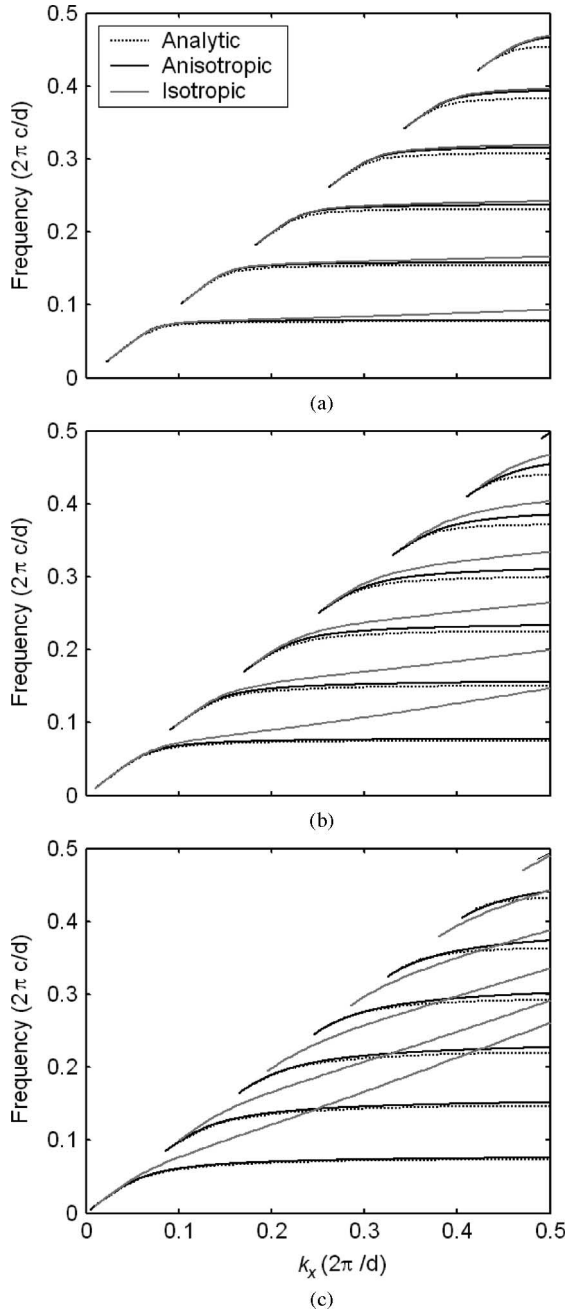


Fig. 2. Waveguide dispersion for metal films with various slit widths. (a) $d/a = 10$ (narrow slit). (b) $d/a = 4$, and (c) $d/a = 2$ (wide slit). The dotted, black solid, and gray solid lines are from the analytic, the anisotropic, and the isotropic models, respectively.

down to around unity. One nontrivial prediction of the metamaterial model is that a metal slab with subwavelength cut-through slits can support guided modes [15]. These modes have fields decaying exponentially outside the slab. Its dispersion relation $\omega(k)$ lies below the light line ($\omega = ck$). Here, we compare the dispersion relation of such guided modes, as predicted by the anisotropic metamaterial model, with those from exact analytic calculations [15] for d/a equal to 10, 4, and 2 (Fig. 2). A good agreement is clearly observed. A similar agreement can be also seen in the transmission spectrum for light externally incident

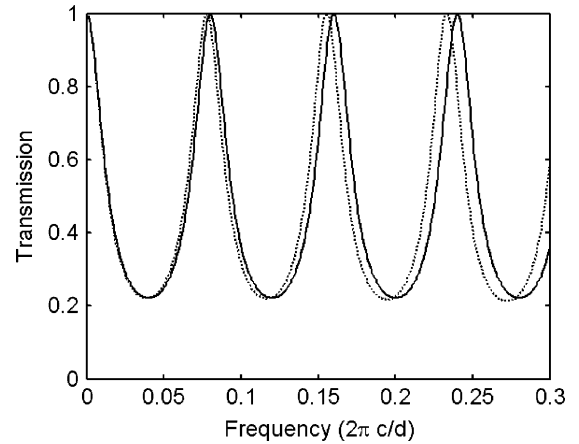


Fig. 3. Transmission of a normally incident plane wave through the metal slit structure with thickness $25d/4$. The dotted and the solid lines are from the analytical and the anisotropic models, respectively.

upon the slab (Fig. 3). This good agreement can be intuitively understood by noting that the electric field inside the metallic system averaged over one period of the structure is exactly the same as the electric field inside the effective medium, for a plane wave with a given k_x . The amplitude is the same and so is the direction (parallel to the interface). Moreover, the wavevector is the same for the two systems, as the normal component of the wavevector does not depend on the transverse component in both the systems and their values are the same since we chose the normal effective index (\bar{n}_{xy}) to be the same as the index of the slit-filling material. In addition, the reflection coefficient of a plane wave at the interface between the system and the surrounding medium is the same, since we have made the impedance the same as well while deriving the anisotropic model. For a symmetric slab structure, most of the electromagnetic characteristics are determined by the round trip phase and the amplitude factor, or equivalently, the wavenumber and the reflection coefficient, for a plane wave propagating inside the slab. From these observations, it can be argued that the anisotropic model is valid for describing the property of the metal slit structures in most physical experiments.

C. Nonuniqueness of the Model

A very unusual characteristic of the anisotropic model, the thickness of the effective medium (\bar{L}) can, in fact, be chosen to have any value, provided that we scale the dielectric and magnetic properties accordingly. Specifically, we can multiply $\bar{\epsilon}_x$, $\bar{\mu}_y$, and $1/\bar{L}$ with an arbitrary real scaling factor s

$$\begin{aligned}\bar{\epsilon}'_x &= s\bar{\epsilon}_x \\ \bar{\epsilon}'_z &= \infty \\ \bar{\mu}'_y &= s\bar{\mu}_y \\ \bar{L}' &= \bar{L}/s\end{aligned}\quad (12)$$

and the resulting effective medium has exactly the same transmission and waveguiding properties. Moreover, the field outside the slab varies identically as a function of distance from the

slab surfaces. Consequently, most electromagnetic experiments would not be able to differentiate between choices of \bar{L} as long as we scale other parameters accordingly.

This scale invariance is a consequence of an infinite $\bar{\epsilon}_z$ and the film geometry. A film structure is unique in the sense that the half space on one side of the film can “communicate” with the other half space on the other side only through the film. Thus, it is not the thickness of the film by itself (\bar{L}), but the round trip phase accumulation ($2\bar{k}_z\bar{L}$), that is of importance. By scaling $\bar{\epsilon}_x$ and $\bar{\mu}_y$ according to \bar{L} , \bar{k}_z is also scaled with the same factor as $\bar{k}_z = \omega\sqrt{\bar{\epsilon}_x\bar{\mu}_y}$ and $\bar{k}_z\bar{L}$ remain the same. The transverse impedance does not change since $\bar{\mu}_y/\bar{\epsilon}_x$ is the same. Hence, the scaling does not affect the outcome of the physical experiments. As all these models are equivalent, in the following discussion for concreteness, the model with $\bar{L} = L$ (2) will be referred to as the anisotropic model.

D. Isotropic Approximation

When d/a is large, the metal structure can be approximated with an isotropic model, as first pointed out in [15]

$$\begin{aligned}\bar{\epsilon}_x &= \left(\frac{d}{a}\right)^2 \\ \bar{\epsilon}_z &= \left(\frac{d}{a}\right)^2 \\ \bar{\mu}_y &= 1 \\ \bar{L} &= \frac{a}{d}L.\end{aligned}\quad (13)$$

As seen in Fig. 2(a), the results from the isotropic model are close to those from the anisotropic model or the actual analytical model when $d/a = 10$. From the discussion on scale invariance, the anisotropic model is equivalent to

$$\begin{aligned}\bar{\epsilon}_x &= (d/a)^2 \\ \bar{\epsilon}_z &= \infty \\ \bar{\mu}_y &= 1 \\ \bar{L} &= \frac{a}{d}L.\end{aligned}\quad (14)$$

Between (13) and (14), the only difference is in the choice of $\bar{\epsilon}_z$, and the difference becomes unimportant when d/a is large. Physically, the electric field inside the isotropic medium is nearly parallel to the interface for large d/a -ratio cases since the continuous quantities are the tangential E field and the normal \mathbf{D} field. Thus, the field configuration is not very different from the anisotropic medium. The isotropic approximation, however, fails to work in the case of smaller d/a ratios, as can be seen in Fig. 2(b) and (c). In these cases, the electric field inside the isotropic model has considerable amount in the normal direction. Also, the wavenumber in the normal direction strongly depends on the tangential wavenumber, while the anisotropic model shows no dependence.

III. COMPARISON OF THE ANISOTROPIC MODEL AND AN ANALYTICAL MODEL

Having shown that the anisotropic model provides a very good description of the slit array system, the focus is now on clarifying its regime of validity by comparing it to the analytical description of the problem. For this purpose, we first show that a set of (ω, k_x) -dependent effective medium parameters can exactly replicate the analytical description, and use them as a reference for checking the validity of the use of nondispersive parameters in the anisotropic model.

As discussed earlier, most of the optical properties of the metal slit film are determined by the wavenumber of the fundamental TEM mode and the mode’s reflection coefficient at the boundary. The choice of effective refractive indices for the anisotropic model is such that the wavenumber inside the effective medium is the same as that of the TEM mode. The same parameter will be used for the reference, dispersive effective medium as well

$$\begin{aligned}n_{zy}^{\text{ref}} &= \infty \\ n_{xy}^{\text{ref}} &= n_c.\end{aligned}\quad (15)$$

The main focus will be on finding the value of the dispersive impedance.

For a given frequency and k_x , a TEM wave inside the slit, incident on the boundary, has a well-defined reflection coefficient, which is, in general, complex. Any complex reflection coefficient can be modeled as a reflection from a boundary between two uniform media. From the reflection coefficient, one can deduce the impedance of one medium provided that the properties of the other medium are known. In other words

$$r = \frac{\eta_2 \frac{k_{z2}}{n_2} - \eta_1^{\text{ref}} \frac{k_{z1}}{n_c}}{\eta_2 \frac{k_{z2}}{n_2} + \eta_1^{\text{ref}} \frac{k_{z1}}{n_c}}\quad (16)$$

can be solved for η_1^{ref}

$$\eta_1^{\text{ref}} = \eta_2 \frac{n_c k_{z2}}{n_2 k_{z1}} \frac{1-r}{1+r}\quad (17)$$

for given $\eta_2, n_2, k_{z2}, n_c, k_{z1}$, and r . (The surrounding medium will be denoted as medium 2, and the dispersive effective medium will be labeled “ref.”) The resulting η_1^{ref} is, in general, complex and depends on the frequency and the incident angle.

To assess the dependence, the form of the reflection coefficient for the metal slit system resulting from the analytical calculation is analyzed. It can be found by expressing the field outside the structure with a superposition of plane waves (diffraction orders due to periodicity), and the inside field with a TEM wave [15]. The resulting expression for the reflection coefficient appears very much like a reflection coefficient from a boundary between uniform media

$$r = \frac{\eta_2 \frac{k_{z2}}{n_2} - \eta_c g k}{\eta_2 \frac{k_{z2}}{n_2} + \eta_c g k}\quad (18)$$

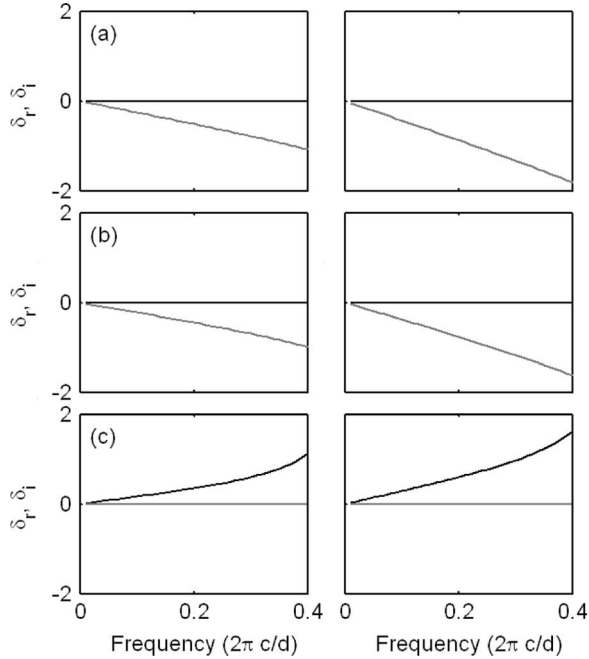


Fig. 4. Real (black) and imaginary (gray) part of the relative impedance correction for (a) normal incidence, (b) oblique incidence, and (c) total internal reflection. The left subpanel is for $d/a = 4$, and the right, 10.

except that the parameter g is dispersive

$$g = f \left[\sin c(f p_0) - i \sum_{p \neq 0} \frac{k_{z2}}{\alpha_p} \sin c(f(p + p_0)) \right]$$

$$f = a/d, \quad p_0 = k_x d/2\pi$$

$$\alpha_p = [(2\pi p/d + k_x)^2 - n_2^2 \omega^2/c^2]^{1/2}. \quad (19)$$

The integer p designates the diffraction order of the modes outside the structure (Only $p = 0$ can be a propagating plane wave for $\lambda > d$), and α_p ($p \neq 0$) is the decaying constant in the z direction for higher order modes. f is the ratio of the slit width a to the period d .

By comparing (16) and (18), the effective impedance is readily found to be

$$\eta_1^{\text{ref}} = \eta_c g. \quad (20)$$

In the low frequency limit ($\lambda \gg d$), $2\pi/d$ is far larger than any of $n_2\omega/c$, k_{z2} , or k_x , assuming that only k_x is being considered, which is of the same order as k_2 . Therefore, k_{z2}/α_p is negligible and $\sin c(f p_0)$ approaches unity. Correspondingly, the effective medium parameter g approaches f . Thus, this more elaborate model gives the same conclusion about the effective impedance and the dispersion as the anisotropic model: $\bar{\eta} = \eta_c f$ and $\bar{k}_z = \bar{n}_{xy} k$, as can be seen in the low frequency limit in Fig. 4.

Without the low frequency approximation, however, the impedance takes a complex value: $\bar{\eta}_t = \eta_c g$ (g is complex). One can better understand the (ω, k_x) dependence of η_1^{ref} by looking at the contributions to the g factor from the zeroth-order

and higher order diffraction waves separately

$$g = f(1 + \delta)$$

$$\delta = \sin c(f p_0) - 1 - i \sum_{p \neq 0} \frac{k_{z2}}{\alpha_p} \sin c(f(p + p_0)). \quad (21)$$

The first two terms in δ arise from the zeroth-order scattering while the third term is due to all higher order scattering. As pointed out earlier, in the long-wavelength limit, δ approaches zero.

The behavior of δ is different in the two regimes (it is assumed that n_c and n_2 are real):

- 1) *Regime 1*: normal or oblique incidence with propagating modes in both the media;
- 2) *Regime 2*: total internal reflection.

In regime 1, k_{z2} is real. Thus, the zeroth-order scattering contributes to the change of the real part of the impedance while higher order scattering leads to the change of the imaginary part. In regime 2, k_{z2} is purely imaginary, hence the correction δ is real. In either regime, it is useful to look at the real part δ_r and the imaginary part δ_i of the relative correction of the effective impedance.

δ_r and δ_i are plotted as a function of frequency in Fig. 4, for three choices of ck_x/ω : 1) normal incidence ($k_x = 0$); 2) oblique incidence below the critical angle ($k_x = 0.5\omega/c$); and 3) total internal reflection ($k_x = 1.2\omega/c$). The left subpanel of each panel is for slits with width $a = 0.25d$, and the right subpanel is for narrower slits ($a = 0.1d$). From the figures, it is evident that, in the low-frequency limit, both δ_r and δ_i converge to zero, and the reference effective medium model can be successfully substituted with the much simpler, dispersionless anisotropic model.

For higher frequencies, the deviation of the effective impedance from the low-frequency value becomes noticeable. In regime 1, the correction is largely imaginary, while, in regime 2, it is entirely real. Regardless of the regime, the relative correction grows larger than unity eventually at high frequencies, and this behavior is the same regardless of the slit width. Thus, for a given wavelength, making the slit narrow alone does not guarantee the validity of the anisotropic model, if the periodicity is not reduced as well.

The sensitivity of different optical properties to the impedance of the film varies widely. For example, the cutoff frequency of the waveguide modes are exactly predicted by the anisotropic model. This is because the impedance deviation in regime 2 is purely real. The cutoff frequency is not affected by the absolute value of a purely real impedance and is solely determined by the thickness and the effective index of the film. In contrast, the curvature of the dispersion curve is strongly influenced by the real-valued impedance correction. Also, the transmission amplitude spectrum is more sensitive to the real part of the impedance correction rather than the imaginary part, especially for films with thickness larger than the period.

In the actual metal slit array structure, there exists a finite E_z field that decays into the metal slit. The effective medium model cannot take this into account. One can think of assigning

a plasmonic form for the $\bar{\epsilon}_z$ to simulate the decaying behavior of E_z , but Maxwell's equations show that $\bar{\epsilon}_z$ is more related to the propagation constant in the x direction and that $\bar{\epsilon}_x$ is responsible for the decaying or propagating behavior in the z direction (6). In other words, the effective medium has only one mode for the same polarization and only one wavenumber for that mode, whether it is real or imaginary. Fortunately, the effect of this decaying E_z is small for most cases, especially when the thickness is not subwavelength.

IV. FINAL REMARKS

The derivation in this paper assumed a perfect conductor, and it is readily applicable to real metals in the microwave frequency range. The other polarization (transverse-electric waves, TE), though not dealt with earlier, can be successfully modeled with a plasmonic form of the dielectric constant

$$\begin{aligned}\bar{\mu}_x &= \frac{8}{\pi^2} \left(\frac{a}{d} \right) \mu_c \\ \bar{\mu}_z &= \infty \\ \bar{\epsilon}_y &= \frac{\pi^2}{8} \left(\frac{d}{a} \right) \left[1 - \frac{\omega_p^2}{\omega^2} \right] \epsilon_c\end{aligned}\quad (22)$$

where $\omega_p (= \pi c/a)$ is the cutoff frequency of the slit. The derivation parallels that of the TM polarization. However, the difference is that the dominant field inside the metal slit is now the lowest order TE wave

$$\begin{aligned}E_y &= E_{y0} \cos\left(\frac{\pi}{a}x\right) e^{-\alpha_z z} \\ H_x &= -i \frac{\alpha_z}{\omega \mu_c} E_{y0} \cos\left(\frac{\pi}{a}x\right) e^{-\alpha_z z} \\ H_z &= i \frac{\pi/a}{\omega \mu_c} E_{y0} \sin\left(\frac{\pi}{a}x\right) e^{-\alpha_z z}.\end{aligned}\quad (23)$$

As for the TM case, the field inside a slit is independent of k_x . A TE wave inside the effective medium can be expressed as

$$\begin{aligned}\bar{E}_y &= \bar{E}_{y0} e^{-\bar{\alpha}_z z} e^{ik_x x} \\ \bar{H}_x &= -i \frac{\bar{\alpha}_z}{\omega \bar{\mu}_x} \bar{E}_{y0} e^{-\bar{\alpha}_z z} e^{ik_x x} \\ \bar{H}_z &= -\frac{k_x}{\omega \bar{\mu}_z} \bar{E}_{y0} e^{-\bar{\alpha}_z z} e^{ik_x x}.\end{aligned}\quad (24)$$

With similar derivations, we obtain

$$\begin{aligned}\bar{\mu}_z &= \infty \\ \bar{\epsilon}_y \bar{\mu}_x &= \epsilon_c \mu_c - \frac{(\pi/a)^2}{\omega^2}.\end{aligned}\quad (25)$$

In this case, $\bar{\mu}_z = \infty$ arises purely from the fact that the dispersion relation in the effective medium as well as the metal slit array is independent of k_x . As a result, in the effective medium, \bar{H}_z is zero, while H_z does not vanish in the slit array. Continuity conditions for the tangential \mathbf{E} field

$$\bar{E}_{y0} = \frac{2}{\pi} \frac{a}{d} E_{y0}\quad (26)$$

and the normal component of Poynting vector

$$\frac{\bar{\alpha}_z}{\omega \bar{\mu}_x} |\bar{E}_{y0}|^2 = \frac{a}{2d} \frac{\alpha_z}{\omega \mu_c} |E_{y0}|^2\quad (27)$$

uniquely determine parameters as shown in (22).

REFERENCES

- [1] M. S. Kushwaha, "Plasmons and magnetoplasmons in semiconductor heterostructures," *Surf. Sci. Rep.*, vol. 41, no. 1–8, pp. 5–416, 2001.
- [2] J. B. Pendry, A. J. Holden, W. J. Stewart, and I. Youngs, "Extremely low frequency plasmons in metallic mesostructures," *Phys. Rev. Lett.*, vol. 76, no. 25, pp. 4773–4776, Jun. 1996.
- [3] D. Felbacq and G. Bouchitte, "Homogenization of a set of parallel fibres," *Waves Random Media*, vol. 7, no. 2, pp. 245–256, Apr. 1997.
- [4] J. B. Pendry, A. J. Holden, D. J. Robbins, and W. J. Stewart, "Low frequency plasmons in thin-wire structures," *J. Phys., Condens. Matter*, vol. 10, no. 22, pp. 4785–4809, Jun. 1998.
- [5] P. A. Belov, C. R. Simovski, and S. A. Tretyakov, "Two-dimensional electromagnetic crystals formed by reactively loaded wires," *Phys. Rev. E, Stat. Phys. Plasmas Fluids Relat. Interdiscip. Top.*, vol. 66, no. 3, p. 036610, Sep. 2002.
- [6] R. Marques, C. R. Martel, F. Mesa, and F. Medina, "Left-handed-media simulation and transmission of EM waves in subwavelength split-ring-resonator-loaded metallic waveguides," *Phys. Rev. Lett.*, vol. 89, no. 18, p. 183901, Oct. 2002.
- [7] B. T. Schwartz and R. Piestun, "Total external reflection from metamaterials with ultralow refractive index," *J. Opt. Soc. Amer. B, Opt. Phys.*, vol. 20, no. 12, pp. 2448–2453, Dec. 2003.
- [8] D. F. Sievenpiper, E. Yablonovitch, J. N. Winn, S. Fan, P. R. Villeneuve, and J. D. Joannopoulos, "3D metallo-dielectric photonic crystals with strong capacitive coupling between metallic islands," *Phys. Rev. Lett.*, vol. 80, no. 13, pp. 2829–2832, Mar. 1998.
- [9] J. B. Pendry, A. J. Holden, D. J. Robbins, and W. J. Stewart, "Magnetism from conductors and enhanced nonlinear phenomena," *IEEE Trans. Microwave Theory Tech.*, vol. 47, no. 11, pp. 2075–2084, Nov. 1999.
- [10] D. R. Smith, W. J. Padilla, D. C. Vier, S. C. Nemat-Nasser, and S. Schultz, "Composite medium with simultaneously negative permeability and permittivity," *Phys. Rev. Lett.*, vol. 84, no. 18, pp. 4184–4187, May 2000.
- [11] D. R. Smith and N. Kroll, "Negative refractive index in left-handed materials," *Phys. Rev. Lett.*, vol. 85, no. 14, pp. 2933–2936, Oct. 2000.
- [12] S. O'Brien and J. B. Pendry, "Magnetic activity at infrared frequencies in structured metallic photonic crystals," *J. Phys., Condens. Matter*, vol. 14, no. 25, pp. 6383–6394, Jul. 2002.
- [13] F. J. Rachford, D. L. Smith, P. F. Loschialpo, and D. W. Forester, "Calculations and measurements of wire and/or split-ring negative index media," *Phys. Rev. E, Stat. Phys. Plasmas Fluids Relat. Interdiscip. Top.*, vol. 66, no. 3, p. 036613, Sep. 2002.
- [14] J. B. Pendry, L. Martin-Moreno, and F. J. Garcia-Vidal, "Mimicking surface plasmons with structured surfaces," *Science*, vol. 305, no. 5685, pp. 847–848, Aug. 2004.
- [15] J. T. Shen, P. B. Catrysse, and S. Fan, "Mechanisms for designing metallic metamaterials with a high index of refraction," *Phys. Rev. Lett.*, vol. 94, no. 19, p. 197401, May 2005.
- [16] F. J. Garcia-Vidal, L. Martin-Moreno, and J. B. Pendry, "Surfaces with holes in them: New plasmonic metamaterials," *J. Opt. A, Pure Appl. Opt.*, vol. 7, no. 2, pp. S97–101, Feb. 2005.

Jonghwa Shin (S'01) received the M.S. degree in electrical engineering in 2003 from Stanford University, Stanford, CA, where he is currently working toward the Ph.D. degree.

In 2001, he carried out research on novel all-optical multi-input logic gates at the Optical Communication Systems Laboratory, Seoul National University, Seoul, Korea. Currently, he is with the Edward L. Ginzton Laboratory, Stanford University. His current research interests include theoretical and computational design and analysis of three-dimensional nanophotonic structures.

Mr. Shin is a Student Member of the Optical Society of America and the Material Research Society. He was the recipient of a scholarship from the Korea Foundation for Advanced Studies. He is one of the first recipients of the Samsung Lee Kun Hee Scholarship.

Jung-Tsung Shen received the Ph.D. degree in physics from the Massachusetts Institute of Technology, Cambridge, in 2003.

Currently, he is a Postdoctoral Researcher at the Edward L. Ginzton Laboratory, Stanford University, Stanford, CA.

Peter B. Catrysse (S'93–M'03) received the “Burgerlijk” Electrotechnical Engineering degree in applied physics from the Vrije Universiteit Brussel, Brussels, Belgium, in 1994. He received the M.S. and the Ph.D. degrees in electrical engineering from Stanford University, Stanford, CA, in 1996 and 2003, respectively.

Since 2003, he has been a Postdoctoral Scholar at the Edward L. Ginzton Laboratory, Stanford University. During 1997–1998, he was with Hewlett-Packard Laboratories, Palo Alto, CA, where he investigated digital camera simulation and high dynamic range imaging. His current research interests include optical sensing, CMOS sensors, nanophotonics, and plasmonics. His research has been concerned with complementary metal-oxide semiconductor image-sensor pixels.

Dr. Catrysse is a member of the Optical Society of America, the Material Research Society, and the International Society for Optical Engineering. He was the recipient of the 1996 Brussels Hoover Fellowship of the Belgian American Educational Foundation, Inc. and a Fund for Scientific Research—Flanders (Belgium) Fellowship in 1998.

Shanhui Fan (M'05–SM'06) received the Ph.D. degree in theoretical condensed matter physics from the Massachusetts Institute of Technology (MIT), Cambridge, in 1997.

Since 2001, he has been an Assistant Professor of Electrical Engineering at Stanford University, Stanford, CA. Earlier, he was a Research Scientist at the Research Laboratory of Electronics at MIT. He is the author or coauthor of 105 journal articles. He has been a prolific speaker and has given 70 invited talks. He is the holder of 19 granted U.S. patents. His current research interests include computational and theoretical studies of solid-state and photonic structures and devices, especially photonic crystals, microcavities, and nanophotonic circuits and elements.

Prof. Fan was the recipient of a National Science Foundation Career Award and a David and Lucile Packard Fellowship in Science and Engineering.